Chemical Science

Accepted Manuscript

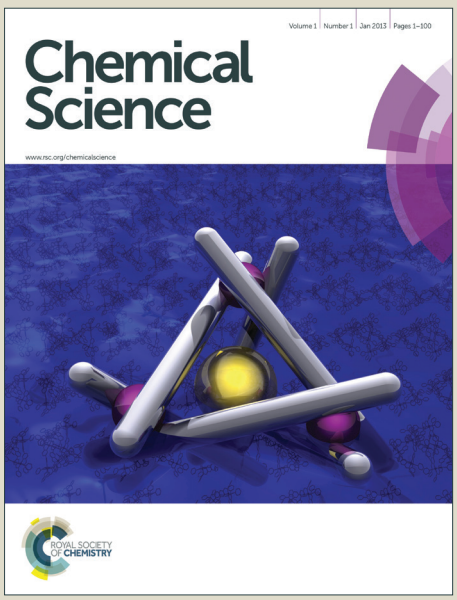

ROYAL SOCIETY OF CHEMISTRY

www.rsc.org/chemicalscience

Chemical Science

RSCPublishing

EDGE ARTICLE

Functionalized graphene-based biomimetic microsensor interfacing with living cells to sensitively monitor nitric oxide release

Yan-Ling Liu, Xue-Ying Wang, Jia-Quan Xu, Chong Xiao, Yan-Hong Liu, Xin-Wei Zhang, Jun-Tao Liu and Wei-Hua Huang*

Cite this: DOI: 10.1039/x0xx00000x

Received ooth January 2012,
Accepted ooth January 2012

DOI: 10.1039/x0xx00000x

www.rsc.org/

It is of great challenge to develop electrochemical sensors with superior sensitivity concurrently possessing high biocompatibility for monitoring at single cell levels. Here we report a novel and reusable biomimetic micro-electrochemical sensor array with nitric oxide (NO) sensing-interface based on metalloporphyrin and 3-aminophenylboronic acid (APBA) co-functionalized reduced graphene oxide (rGO). The assembling of high specifically catalytic but semi-conductive metalloporphyrin with high electric conductive rGO confers the sensor with sub-nanomolar sensitivity. Further coupling with the small cell-adhesive molecule APBA obviously enhances the cytocompatibility of the microsensor without diminishing the sensitivity, and the reversible formation between APBA and cell membrane carbohydrates allows practical reusability. The microsensor was successfully used to sensitively monitor in real time NO molecule release from human endothelial cells being cultured thereon, demonstrating its potential application in detection of NO with very low bioactive concentrations for better understanding of its physiological functions and medical tracking of patient state.

Introduction

Nitric oxide (NO) has attracted intense interest owing to its diverse and vital roles in the regulation of physiological processes, such as cardiovascular systems, neurotransmission, immune responses and angiogenesis.[1-6] Quantification of NO *in vivo* is indispensable to comprehensively unravel its function in physiology. However, measuring NO in biological systems is challenging due to its short half-life (< 10 s), trace level (physiological range of NO bioactivity is as low as 100 pM or below) and complex interfering species.[7-11] Methods commonly available including chemiluminescence, absorbance, fluorescence and electron paramagnetic resonance spectroscopy,[12-15] suffer from high cost or complicated pretreatment that restricts real-time measurement. Although newly developed technique such as field-effect transistor or surface enhanced Raman spectroscopy allows real-time detection of NO outside or inside living cells,[16, 17] electrochemical NO sensor, especially based on microelectrodes, due to its ultra-fast response time, high-spatial resolution and non-invasive size enables it to be a powerful tool for direct and real-time monitoring of NO release in physiology.[7, 18-22]

In the past decades, great efforts have been made to ensure the electrochemical sensors with sufficient sensitivity and selectivity to accurately detect NO. To improve sensor sensitivity, different types of catalytic materials, such as metalloporphyrin (phthalocyanine and salen),[23-25] carbon nanotube,[26] metal nanoparticles and nanowires,[27-29] have been employed to develop sensitive NO sensors. With unique properties, graphene has emerged to be a rising star material and advanced the development of electrochemistry.[30-32] Recently, graphene has shown great potential for sensitive detection of NO.[33-35] Moreover, enhanced selectivity was achieved by coating permselective membrane on the sensor.[7, 21, 22] Nafion, Teflon and o-phenylenediamine are often used to restrict the diffusion of interferent molecules (e.g., nitrite, ascorbic acid and dopamine) to the electrode surface.[23, 36, 37]

Comparing with isolated cell and its above electrode configuration, culturing cells on microelectrodes could better reconstruct the *in vivo* interface between NO emitting cells and their receptor cells (e.g., endothelium and smooth muscle cells), and monitoring of NO from the tightly attached cells could therefore closely approach the real physiological conditions. In this case, biocompatibility is a critical issue that should be seriously considered. Pre-coating of positively charged polyelectrolytes (e.g., poly-l-lysine[38]) or extracellular matrix

Key Laboratory of Analytical Chemistry for Biology and Medicine (Ministry of Education), College of Chemistry and Molecular Sciences, Wuhan University, Wuhan, 430072, China. E-mail: whhuang@whu.edu.cn; Fax: +86-27-68754067;Tel: +86-27-68752149

Electronic supplementary information (ESI) available: detailed experimental procedures and materials; Fig S1-Fig S10 and Table S1. See DOI: 10.1039/b000000x

(e.g., laminin[39] and collagen[40]) are typically utilized to boost cell attachment. However, the additional polymer and extracellular matrix for selectivity or biocompatibility enhancement will actually decrease electrode response,[7, 17, 41] and it was quite difficult to coat very small or irregularly shaped electrode surfaces in a controlled way. Lately, small cell-adhesive molecules, such as RGD and monosaccharides,[34 41] have been explored to interface electrodes with living cells, providing an approach of fabricating biocompatible sensors.

So far, great successes have been achieved in developing NO electrochemical sensors with sensitivity above nanomolar concentrations. However, construction of sensing-interfaces with sub-nanomolar to picomolar sensitivity while concurrently possessing excellent cytocompatibility and high selectivity still remains a great challenge, especially for high throughput detection at single cell levels (i.e., single or a few cells). Herein, we developed a multifunctional microsensor array for detection of NO from several cells. Inspired by the excellent catalysis of metalloporphyrin to NO electrooxidation and the two-dimensional nanostructure and high electric conductivity of graphene, we prepared a novel hybrid nanosheets based on Fe (III) meso-tetra (4-carboxyphenyl) porphyrin (FeTCP) and reduced graphene oxide (rGO) through the π-π interaction, named FGHNs, which was modified onto ITO microelectrode array via electrophoretic deposition. FGHNs was further covalently functionalized with a small cell-adhesive molecule 3-aminophenylboronic acid (APBA), which can react with 1,2- or 1,3-diols of moieties in carbohydrates existing largely on the cell membrane,[42-45] to enable the sensor with good cytocompatibility. As-prepared microsensor array and the electroactive area are schematically shown in Scheme 1. The microsensor demonstrated exceptional sensitivity and selectivity to NO with a detection limit of 55 pM in PBS and 90 pM in cell medium, and human umbilical vein endothelial cells (HUVECs) can adhere and proliferate well on the electrode surface, therefore promoting interface with living cells being cultured thereon and high sensitive real-time monitoring of NO release.

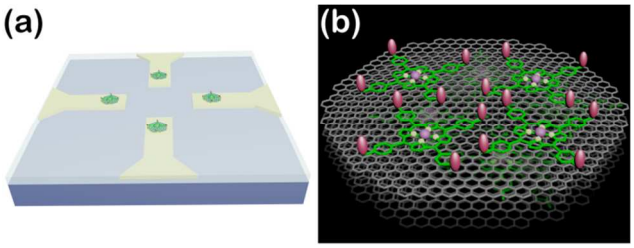

Scheme 1 (a) Schematic of the APBA/FGHNs/ITO microelectrode array (only 4 microelectrodes are shown here for simplicity). (b) Schematic illustration of APBA/FGHNs in the active electrode area, and the gray, green and pink diagrams represent rGO, FeTCP and APBA, respectively.

Results and discussion

Preparation and characterization of the FGHNs sheets

The nanosheets FGHNs was prepared by a procedure similar to that previously reported.[46] Briefly, water-soluble GO and FeTCP were ultrasonically mixed to promote the π-π interaction between them, then hydrazine hydrate was added to the above solution for reducing GO (see Methods in ESI). As shown in Fig 1a, a stable FGHNs dispersion was obtained (Fig 1a, inset III) after hydrazine reduction, and the peak at 226 nm of GO attributing to the π-π* transition of aromatic C=C bonds shifts to 261 nm belonging to rGO.[47] The new absorption at 423 nm was also observed, which corresponds to the Soret band of FeTCP with a red shift (27 nm).[46-48] The results indicate FeTCP was adsorbed on the surface of rGO sheets by π-π interactions. Meanwhile, compared with FGHNs, the dispersion of rGO without the stabilization of FeTCP lead to the aggregation of rGO sheets after reduction (Fig 1a, inset II). The attachment of FeTCP on rGO surface was also characterized by electrochemical method. Fig 1b shows the cyclic voltammograms of bare ITO (blue line), FeTCP/ITO (purple line), rGO/ITO (red line), FGHNs/ITO (black line) in 0.1 M phosphate buffered saline (PBS). Compared with ITO and rGO/ITO, a pair of redox peaks was observed in the potential range from -0.6 V to 0.0 V by FGHNs/ITO. The redox peaks obviously should belong only to FeTCP in FGHNs, which is the characteristic of electron transfer process of iron at the core of Fe (III) TCP/Fe (II) TCP (Fig 1b, purple line). Further, AFM result shows that the average thickness of single-layer FGHNs was determined to be about 1.45 nm (Fig 1c). There was 0.80-nm increment compared with that of pure rGO, the single-layer thickness of which is *ca*. 0.65 nm,[47] owing to the presence of FeTCP on the rGO sheet surfaces. Thus the thickness of FeTCP layer was calculated to be about 0.40 nm since FeTCP could locate on both sides of the rGO.[49, 50]

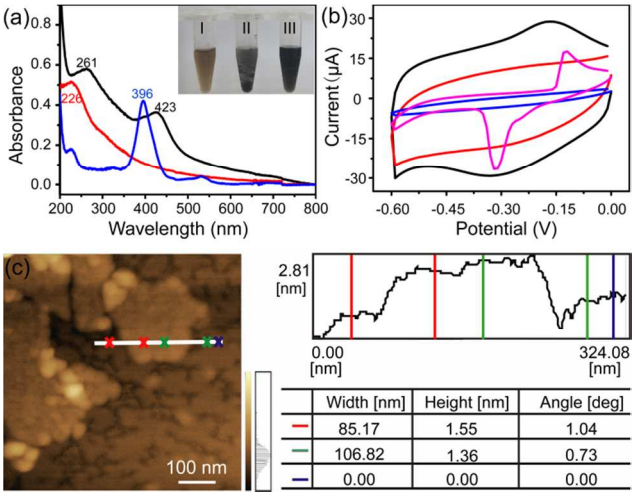

Fig.1 (a) UV-visible spectra of FeTCP solution (blue line), GO suspension (red line) and FGHNs suspension (black line). Inset: photographs of GO (I), rGO (II) and FGHNs (III) dispersed in water. (b) Cyclic voltammograms of bare ITO (blue line), FeTCP/ITO (purple line), rGO/ITO (red line), FGHNs/ITO (black line) in 0.1 M PBS saturated with N_2 at a scan rate of 50 mV s^{-1}. (c) AFM image of FGHNs.

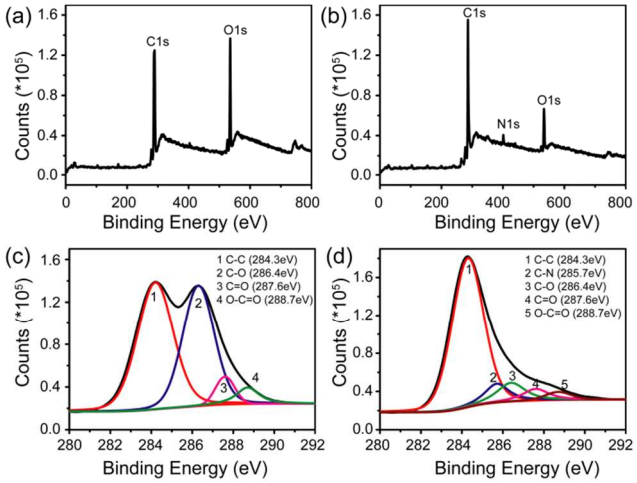

Fig.2 XPS data for (a) GO and (b) FGHNs. The deconvolution of C1s spectra of (c) GO and (d) FGHNs.

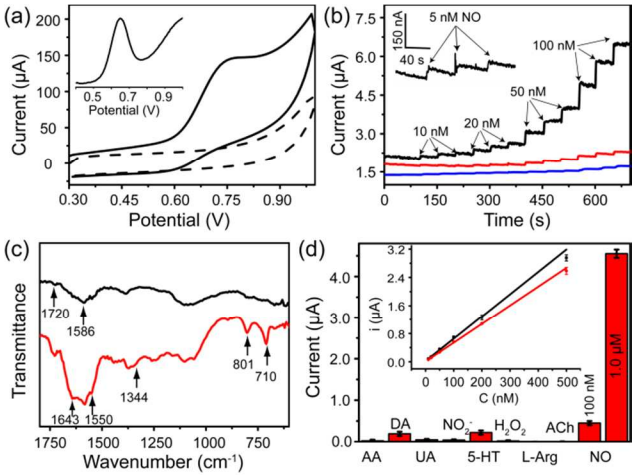

Fig.3 (a) Cyclic voltammograms of FGHNs/ITO in the absence (dash line) and presence (solid line) of 10 μM NO in deaerated PBS solution at a scan rate of 50 mV s^{-1}. Inset: differential pulse voltammogram of FGHNs/ITO to 10 μM NO. (b) Amperometric curves of FeTCP/ITO (blue line), rGO/ITO (red line), FGHNs/ITO (black line) to a series of NO concentration increases in a stirred deaerated PBS solution and the response of FGHNs/ITO to 5 nM NO is magnified in the inset. A potential of +0.75 V (vs. Ag/AgCl) was applied to all the electrodes. (c) ATR-IR spectra of FGHNs (black line) and APBA/FGHNs (red line). (d) Selective profile of the APBA/FGHNs/ITO to interferences in cell medium RPMI 1640, in which all interfering species were at the concentration of 2 μM. Inset: calibration curves of FGHNs/ITO (black line) and APBA/FGHNs/ITO (red line) for increasing NO concentration in cell medium.

X-ray photoelectron spectroscopy (XPS) was employed to further explore the interaction between rGO and FeTCP. Compared with GO (Fig 2a), the survey of FGHNs shows the presence of detectable amounts N1s at about 400 eV, originating from FeTCP, indicating the functionalization of rGO by FeTCP successfully occurred (Fig 2b). After hydrazine reduction, the C1s spectrum indicates the peaks associated with C-C or C-H (284.3 eV) became predominant, while the peaks related to the oxidized carbon species (C-O, C=O) were greatly weakened (Fig 2c, d). Meanwhile, a new peak appears at 285.7 eV in the spectra of FGHNs, belonging to the carbon in the C-N bonds. These results indicate that GO has been well deoxygenated into rGO which were further protected by FeTCP molecules to form FGHNs.

Electrochemical behaviors of FGHNs and APBA/FGHNs

The FGHNs/ITO exhibited excellent electrochemical behavior to NO (the standard solution was prepared as previously described[26]) and the differential pulse and cyclic voltammograms showed a peak at +0.65 V and +0.75 V (Fig 3a), respectively. It is worth noting that FGHNs/ITO acted as the best catalyst compared with rGO/ITO and FeTCP/ITO (Fig 3b), the sensitivities of which were calculated to be 37.6, 7.2 and 2.1 $\mu A \cdot \mu M^{-1} \cdot cm^{-2}$, respectively. Metalloporphyrin was widespreadly used as specifically catalytic coatings for construction of NO electrochemical sensors,[7,21,23] but it has poor electrical conductivity. The introduction of underlying rGO greatly enhanced the catalytic capability to NO by affording a high-conductive bridge to facilitate rapid electron transport between porphyrin and the electrode.[48, 50] This attributes to amazingly synergistic electrooxidation to NO.

FGHNs/ITO was further covalently functionalized with small cell-adhesive molecule APBA by coupling -COOH and -NH_2 in FeTCP and APBA. Attenuated Total Reflection Infrared Spectroscopy (ATR-IR) of FGHNs displayed two peaks at 1720 and 1586 cm^{-1} (Fig 3c, black line), which should be assigned to the stretch mode of a carboxyl group in FeTCP. After the covalent bonding of APBA with FGHNs, two new peaks at 1643 and 1550 cm^{-1} corresponding to the characteristic amine groups were observed (Fig 3c, red line). In addition, the presence of the B-O stretching mode at 1344 cm^{-1}, together with clearly aromatic C-H stretching at 801 and 710 cm^{-1}, further evidenced successful immobilization of APBA.

Besides, the comparison of electrochemical responses in PBS solution (data not shown) and cell medium (Fig S1) were also investigated, and the average sensitivities of APBA/FGHNs/ITO in the both conditions remain more than 80% (the ratio of the calibration curve slopes) of that FGHNs/ITO after its further functionalization and reuse (Fig 3d, inset), indicating the unobvious influence of small cell-binding molecule APBA to the response of electrodes. The selectivities of FGHNs/ITO and APBA/FGHNs/ITO toward NO in PBS were studied by investigating interferents such as ascorbic acid (AA), dopamine (DA), uric acid (UA), NO_2^- (Fig S2). The calculated selectivity ratios for NO against AA, DA, UA and NO_2^- were 89, 74, 111 and 89 for FGHNs/ITO, and 113, 96, 158 and 117 for APBA/FGHNs/ITO, indicating that FGHNs/ITO possesses good selectivity against these interferents, especially negatively charged molecules, and APBA/FGHNs/ITO has better performance than the former. The good selectivity might originate from the highly inherent specificity of metalloporphyrin to the electrocatalytic oxidation of NO, and retained surface carboxyl groups together with boronate of APBA/FGHNs further enhanced the selectivity.

To further demonstrate the selectivity of the sensor in physiological solutions, we also conducted the measurements in cell culture medium RPMI 1640 containing serum (Fig 3d). Besides above-mentioned AA, DA, UA and NO_2^-, other potential interferents including 5-hydroxy tryptamine (5-HT), H_2O_2, L-arginine (L-Arg) and acetylcholine (ACh) were tested (Fig S3), and the concentration of each interferent was 2 μM. The sensor also exhibited practical selectivity against most molecules, except positively charged DA and 5-HT with small detectable signal. In addition, the response of the sensor remains about 90% of the initial current after 10 measurements, indicating high reproducibility of the sensor.

Cell adhesion and proliferation on biomimetic APBA/FGHNs flim

Construction of cell-compatible sensing interface on which cells could be immobilized and grow directly is of great importance to detect cell-released molecules accurately, especially for those that are labile and could be metabolized rapidly, for example, free radical NO. APBA is a molecule capable of specifical binding with 1,2- or 1,3-diols existing widely in carbohydrates of the cell membrane,[42-46] therefore it can be employed as an artificial carbohydrate–receptor for cells adhesion. After being seeded on different substrates with the same cell density and cultured for 1 h, the cells were then rinsed with physiological saline solution for three times to remove cells loosely bounded. It was observed that the number of HUVECs left on APBA/FGHNs/ITO was the biggest (Fig S4), indicating the powerful cell-adhesive capacity of APBA/FGHNs. Besides, the behavior of cell proliferation was also investigated by counting numbers of HUVECs cultured for 1 h, 12 h, 24 h, 36 h, 48 h and 72 h (Fig 4a), until they proliferated and covered almost all over the electrode. Then the cell viability was characterized by fluorescent live/dead cell markers Calcein-AM and PI after being cultured for up to 86 h, and cells were almost clearly alive (Fig 4b), further displaying the excellent cytocompatibility of APBA/FGHNs.

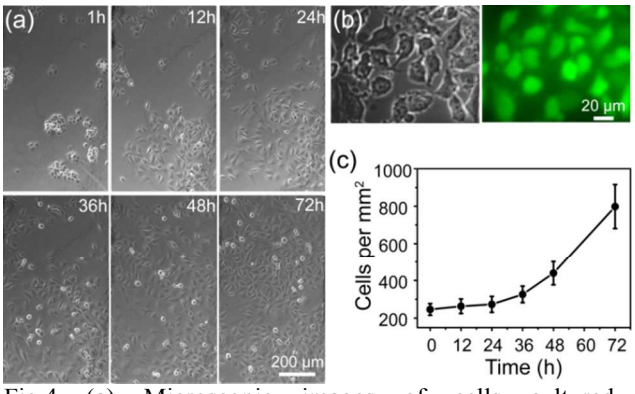

Fig.4 (a) Microscopic images of cells cultured on APBA/FGHNs/ITO for different time. (b) Microscopic photographs of HUVECs cultured for 86 h and labeled with Calcein-AM (green) and PI (red). (c) Proliferation curve of HUVECs cultured on APBA/FGHNs/ITO.

Microelectrode array fabrication and NO release monitoring

To realize real-time monitoring of NO release at single cell levels, we fabricated patterned ITO microelectrode (100 μm in diameter) array using photolithography techniques (see Methods section in ESI, and the process was illustrated in Fig S5).[51] Then FGHNs and APBA was deposited on the microelectrode by electrophoresis and covalent linkage, respectively (see Methods section in ESI, and the electrode morphologies of ITO and APBA/FGHNs/ITO microsensor were shown in Fig S6). To simulate the cell-microsensor configuration during electrochemical detection of NO release, a fast (*ca* 5 s) injection of different concentrations of NO solution filled in a micro-capillary (150 μm in internal diameter, closely near the active area of the electrode) was performed in PBS and cell medium and the results were shown in Fig S7, Fig 5a and Fig S8, respectively. The sensitivity of APBA/FGHNs/ITO microelectrode in RPMI 1640 (0.089 nA/nM, Fig S8) was about 70% of that in PBS solution (0.1232 nA/nM, Fig S7), which perhaps was the result of partial absorption of undesired compounds in cell medium onto the active surface of the microelectrode. The typical response time of this sensor to NO was about 400 ms (Fig. S7a, inset) and 600 ms in PBS and cell medium (Fig. 5a, inset), if we define the response time as the interval between the instant at which current reaches 10% of the maximum and the instant at which current rises to 90% of the maximum. The fast response characteristic of the sensor facilitates the real-time monitoring of NO release from cells. The detection limit was calculated to be about 55 pM in PBS and 90 pM in cell medium (S/N = 3), being the lowest of those reported previously as we known (Table S1).

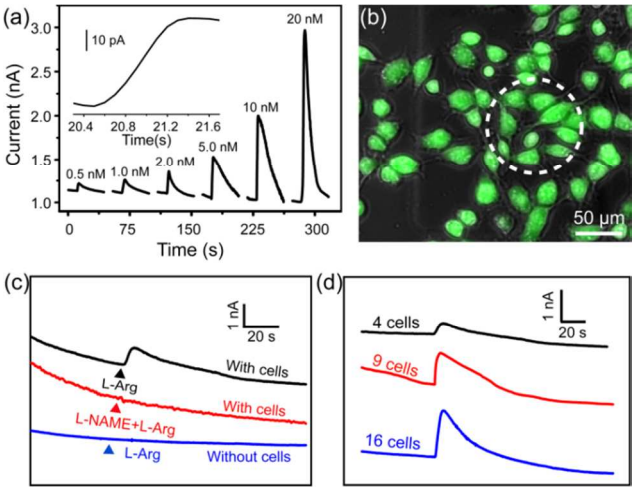

Fig.5 (a) Amperometric curve of APBA/FGHNs/ITO microelectrode to a series of NO concentration increases in RPMI 1640 cell culture medium at a potential of +0.75 V. Inset: an amplified amperometric curve illustrating the response time of the sensor to NO. (b) The microscopic image of the Calcein-AM (green) and PI (red) stained HUVECs cultured on APBA/FGHNs/ITO microelectrode. Active surface area of an individual microsensor was labeled by a white dotted circle. (c) Typical response of APBA/FGHNs/ITO at different conditions (d) Amperometric responses of microelectrodes to 4 (black line), 9 (red line) and 16 (blue line) HUVECs stimulated by L-Arg in RPMI 1640 cell medium.

After seeded on the APBA/FGHNs/ITO microelectrode array, HUVECs grew and proliferated well (Fig S9) and higher cell density was formed on the active microelectrode surface 10 h later. Fluorescent imaging by live/dead cell markers Calcein-AM and PI demonstrated the excellent viability of the cell (Fig 5b). Then the APBA/FGHNs/ITO microsensor was used to monitor NO release from the living cells (Fig 5c, black line) cultured thereon. The production of NO was evoked by stimulating HUVECs with fast injection (1 μL) of 3 mM L-Arg, which can be enzymatically oxidated by nitric oxide synthase (NOS) to produce NO in endothelial cells. Control experiments were carried out to confirm the change in the measured current was due to the oxidation of NO released from HUVECs. When L-Arg was injected onto microelectrodes without cells cultured thereon or cells were simultaneously stimulated with a specific NOS inhibitor L-NAME (100 μM) and L-Arg, no increase in current was detected in the above two conditions (Fig 5c, blue line and red line), excluding the possibilities of L-Arg disturbance and other related electrochemical active interferences. NO release from different number of living cells were monitored by the sensor in both PBS (Fig S10) and cell medium (Fig 5d). Obvious increases in current were observed, which were followed by a gradual decrease of the current to the baseline, and the current amplitude was raised with the increasing number of cells cultured on the sensor. We quantified the average concentration of released NO in cell medium when all the active surface of microelectrode was covered by HUVECs, and the quantitative value was calculated to be about 16 nM, in the range of NO released by endothelial NO synthase.[17, 53]

To test the reusability of the microsensor array after cell culture and NO detection, we detached the attached cells and cell-secreted glycoprotein by firstly immersing it in 0.01 M aqueous NaOH solution then rinsing in water. It was observed that the attached cells could be easily detached away from the sensor for subsequent cell culture and measurement owing to the pH-dependent reversible formation between boronate and carbohydrates. Electrochemical results showed that the microsensor remained over 80% of its initial response after cell detection and sensor renewal for 5 times, indicating a highly promising strategy for constructing reusable cell biosensors especially obtained by complicated microfabrication.

Conclusions

Summarily, we have constructed a multifunctional NO microsensor array based on boronic acid and metalloporphyrin co-functionalized graphene oxide. The hybrid material FGHNs exhibited excellent sensitivity to sub-nanomolar range NO and APBA conferred the sensor with high cytocompatibility to cells and practicable reusability. The sensor was further used for sensitively and selectively real-time monitoring of NO molecule release from attached human endothelial cells in cell culture medium. In addition, the sensor was transparent and could be coupled to optical imaging techniques. Though detection of NO at very low bioactive concentrations under *in vivo* physiological conditions has not yet demonstrated in this work, the exceptional sensitivity, excellent cytocompatibility and reusability of this sensor make it a promising sensing interface to be incorporated into integrated microfluidic or implantable devices, therefore facilitating real-time monitoring of NO at extremely low concentrations in its diverse physiological and pathological conditions with high spatiotemporal resolution.

Acknowledgements

This work was supported by the National Science Foundation of China (Nos. 21375099, 91017013), Specialized Research Fund for the Doctoral Program of Higher Education (20120141110031) and the Fundamental Research Funds for the Central Universities (2042014kf0192).

Notes and references

1. L. J. Ignarro, G. M. Buga, K. S. Wood, R. E. Byrns, G. Chaudhuri, *Proc. Nat. Acad. Sci. U. S. A.*, 1987, **84**, 9265-9269.
2. A. R. Butler, D. L. H. Williams, *Chem. Soc. Rev.*, 1993, **22**, 233-241.
3. F. Murad, *Angew. Chem. Int. Edit*., 1999, **38**, 1856-1868.
4. C. Bogdan, *Nat. Immunol.*, 2001, **2**, 907-916.
5. F. Guix, I. Uribesalgo, M. Coma, F. Munoz, *Prog. Neurobiol.*, 2005, **76**, 126-152.
6. D. D. Thomas, L. A. Ridnour, J. S. Isenberg, W. Flores-Santana, C. H. Switzer, S. Donzelli, P. Hussain, C. Vecoli, N. Paolocci, S. Ambs, *Free Radical Biol. Med.*, 2008, **45**, 18-31.
7. F. Bedioui, N. Villeneuve, *Electroanalysis*, 2003, **15**, 5-18.
8. E. M. Hetrick, M. H. Schoenfisch, *Annu. Rev. Anal. Chem.*, 2009, **2**, 409-433.
9. C. N. Hall, J. Garthwaite, *Nitric Oxide,* 2009, **21**, 92-103.
10. A. M. Batchelor, K. Bartus, C. Reynell, S. Constantinou, E. J. Halvey, K F. Held, W. R. Dostmann, J. Vernon, J. Garthwaite, *Proc. Nat. Acad. Sci. U. S. A.*, 2010, **107**, 22060-22065.
11. K. F. Held, W. R. Dostmann, *Front. Pharmacol.*, 2012, **3(130)**, 1-10.
12. J. K. Robinson, M. J. Bollinger, J. W. Birks, *Anal. Chem*., 1999, **71**, 5131-5136.
13. E. M. Boon, M. A. Marletta, *J. Am. Chem. Soc.*, 2006, **128**, 10022-10023.
14. E. Sasaki, H. Kojima, H. Nishimatsu, Y. Urano, K. Kikuchi, Y. Hirata, T. Nagano, *J. Am. Chem. Soc.*, 2005, **127***,* 3684-3685.
15. N. Hogg, *Free Radical Biol. Med*., 2010, **49**, 122-129.
16. P. Rivera-Gil, C. Vazquez-Vazquez, V. Giannini, M. P. Callao, W. J. Parak, M. A. Correa-Duarte, R. A. Alvarez-Puebla, *Angew. Chem. Int. Edit*., 2013, **52**, 13694-13698.
17. S. Jiang, R. Cheng, X. Wang, T. Xue, Y. Liu, A. Nel, Y. Huang, X. Duan, *Nat. Commun.*, 2013, **4**:2225, doi:10.1038/ncomms3225.
18. A. Schulte, W. Schuhmann, *Angew. Chem. Int. Edit*., 2007, **46**, 8760-8777.
19. I. R. Davies, X. Zhang, *Methods Enzymol.*, 2008, **436**, 63-95.
20. C. Amatore, S. Arbault, M. Guille, F. Lemaître, *Chem. Rev*., 2008, **108**, 2585-2621.
21. B. J. Privett, J. H. Shin, M. H. Schoenfisch, *Chem. Soc. Rev.*, 2010, **39**, 1925-1935.
22. F. Bedioui, S. Griveau, *Electroanalysis*, 2013, **25**, 587-600.
23. T. Malinski, Z. Taha, *Nature*, 1992, **358**, 676-678.

24. S. L. Vilakazi, T. Nyokong, *J. Electroanal. Chem.*, 2001, **512**, 56-63.
25. L. Mao, K. Yamamoto, W. Zhou, L. Jin, *Electroanalysis*, 2000, **12**, 72-77.
26. F. Du, W. Huang, Y. Shi, Z. Wang, J. Cheng, *Biosens. Bioelectron.*, 2008, **24**, 415-421.
27. A. Yu, Z. Liang, J. Cho, F. Caruso, *Nano Lett.*, 2003, **3**, 1203-1207.
28. C. Amatore, S. Arbault, Y. Bouret, B. Cauli, M. Guille, A. Rancillac, J. Rossier, *ChemPhysChem*, 2006, **7**, 181-187.
29. L. M. Li, X. Y. Wang, L. S. Hu, R. S. Chen, Y. Huang, S. J. Chen, W. H. Huang, K. F. Huo, P. K. Chu, *Lab Chip*, 2012, **12**, 4249-4256.
30. Y. Shao, J. Wang, H. Wu, J. Liu, I. A. Aksay, Y. Lin, *Electroanalysis,* 2010, **22**, 1027-1036.
31. D. A. Brownson, D. K. Kampouris, C. E. Banks, *Chem. Soc. Rev.*, 2012, **41**, 6944-6976.
32. S. X. Wu, Q. Y. He, C. L. Tan, Y. D. Wang, H. Zhang, *Small*, 2013, **9**, 1160-1172.
33. W. W. Li, X. M. Geng, Y. F. Guo, J. Z. Rong, Y. P. Gong, L. Q. Wu, X. M. Zhang, P. Li, J. B. Xu, G. S. Cheng, *ACS Nano*, 2011, **5**, 6955-6961.
34. C. X. Guo, S. R. Ng, S. Y. Khoo, X. Zheng, P. Chen, C. M. Li, *ACS Nano*, 2012, **6**, 6944-6951.
35. X. L. Zan, Z. Fang, J. Wu, F. Xiao, F. W. Huo, H. W. Duan, *Biosens. Bioelectron.*, 2013, **49**, 71-78.
36. Y. Lee, J. Kim, *Anal. Chem*., 2007, **79**, 7669-7675.
37. M. N. Friedemann, S. W. Robinson, G. A. Gerhardt, *Anal. Chem.*, 1996, **68**, 2621-2628.
38. L. M. Li, W. Wang, S. H. Zhang, S. J. Chen, S. S. Guo, O. Français, J. K. Cheng, W. H. Huang, *Anal. Chem.*, 2011, **83**, 9524-9530.
39. J. T. Robinson, M. Jorgolli, A. K. Shalek, M.-H. Yoon, R. S. Gertner, H. Park, *Nat. Nanotechnol.*, 2012, **7**, 180-184.
40. J. Wang, R. l. Trouillon, Y. Lin, M. I. Svensson, A. G. Ewing, *Anal. Chem*., 2013, **85**, 5600-5608.
41. H. G. Sudibya, J. Ma, X. Dong, S. Ng, L. J. Li, X. W. Liu, P. Chen, *Angew. Chem. Int. Edit*., 2009, **48**, 2723-2726.
42. A. Monzo, G. K. Bonn, A. Guttman, *TrAC, Trends Anal. Chem.*, 2007, **26**, 423-432.
43. X. Zhong, H. J. Bai, J. J. Xu, H. Y. Chen, Y. H. Zhu, *Adv. Funct. Mater.*, 2010, **20**, 992-999.
44. S. Jin, Y. Cheng, S. Reid, M. Li, B. Wang, *Med. Res. Rev.*, 2010, **30**, 171-257.
45. S. Park, J. C. Gildersleeve, O. Blixt, I. Shin, *Chem. Soc. Rev.*, 2013, **42**, 4310-4326.
46. L. Feng, L. Wu, J. Wang, J. Ren, D. Miyoshi, N. Sugimoto, X. Qu, *Adv. Mater.*, 2012, **24**, 125-131.
47. Y. Guo, L. Deng, J. Li, S. Guo, E. Wang, S. Dong, *ACS Nano*, 2011, **5**, 1282-1290.
48. Y. Xu, L. Zhao, H. Bai, W. Hong, C. Li, G. Shi, *J. Am. Chem. Soc.*, 2009, **131**, 13490-13497.
49. H. Y. Wang, D. X. Han, N. Li, K. A. Li, *J. Inclusion Phenom. Macrocyclic Chem*., 2005, **52**, 247-252.
50. T. Xue, S. Jiang, Y. Qu, Q. Su, R. Cheng, S. Dubin, C. Y. Chiu, R. Kaner, Y. Huang, X. Duan, *Angew. Chem. Int. Edit.*, 2012, **51**, 3822-3825.
51. W. Zhan, J. Alvarez, R. M. Crooks, *J. Am. Chem. Soc.*, 2002, **124**, 13265-13270.
52. R. M. J. Palmer, D. S. Ashton, S. Moncada, *Nature*, 1988, **333**, 664-666.
53. J. Goretski, T. C. Hollocher, *J. Biol. Chem.,* 1988, **263**, 2316-2323.

TOC

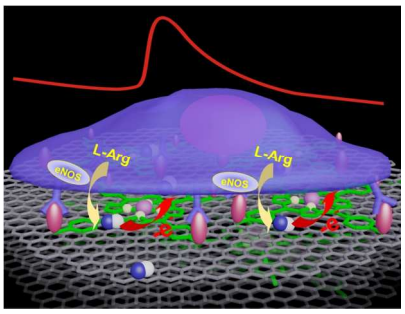

We present a biomimetic and reusable microsensor with sub-nanomolar sensitivity by elaborate functionlizing graphene for monitoring NO release in real-time.